A Wavelet Operational Matrix Approach for Solving a Nonlinear Mixed Type Fractional Integro-Differential Equation

Habibollah Saeedi[1*], Mahmoud Mohseni Moghadam[1,2]

[1]Department of Applied Mathematics, Faculty of Mathematics and Computer, Shahid Bahonar University of Kerman, Kerman, Iran, 76169-14111.
[2]Department of Mathematics, Islamic Azad University of Kerman, Kerman, Iran
[*]Corresponding author email: saeedi@uk.ac.ir.

***Abstract*:** In this paper, an effective operational method will be used to determine the numerical solution of a specific Nonlinear Fractional Volterra-Fredholm integro-differential (NFVFID) equation. The method is based on CAS wavelets and Block Pulse Functions (BPFs) and their operational matrices. The main characteristic of this approach is to reduce a NFVFID equation to a system of algebraic equations, which greatly simplifies the problem. Also some numerical examples are provided to illustrate the accuracy and computational efficiency of the method.

***Keywords*:** Fractional Calculus; CAS Wavelets; Block Pulse Functions; Operational Matrix.

1. Introduction

The aim of this work is to present a numerical method for approximating the solution of the following Nonlinear Fractional Volterra-Fredholm Integro-Differential (NFVFID) equation:

$$D^{\alpha} f(x) - \lambda_1 \int_0^1 k_1(x,t) F_1(t, f(t)) dt - \lambda_2 \int_0^x k_2(x,t) F_2(t, f(t)) dt = g(x), \quad (1)$$

with supplementary conditions:

$$f^{(i)}(0) = f_i,\ i = 0,1,\ldots,r-1,\ r-1 < \alpha \le r,\ r \in \mathbb{N}, \quad (2)$$

where D^{α} is the Caputo fractional differentiation operator, parameters λ_1, λ_2 and functions $k_1(x,t), k_2(x,t), F_1(t, f(t)), F_2(t, f(t))$ and $g(x)$ are given functions in $L^2[0,1)^2$ and $L^2[0,1)$, respectively, and $f(x)$ is the unknown function. Here, we assume that $F_1(t, f(t)) = f^{q_1}(t)$ and $F_2(t, f(t)) = f^{q_2}(t)$, where q_1 and q_2 are positive integers.

In recent years, it has turned out that many phenomena in signal processing, control engineering [1, 2], electromagnetism [3], biosciences [4], fluid mechanics [5], electrochemistry [6], diffusion processes [7], dynamic of viscoelastic materials [8], continuum and statistical mechanics [9] and propagation of spherical flames [10] can be successfully modelled by the use of fractional derivatives and integrals. It is well known that the fractional order differential and integral operators are non-local operators. This is one reason why fractional differential operators provide an excellent instrument for description of memory and hereditary properties of various physical processes. Motivated by increasing number of applications of fractional differential equations, considerable attention has been given to provide efficient methods for exact and numerical solutions of fractional differential equations.

In general, most of the fractional integro-differential equations do not have exact solutions. Particularly, there is no known method for solving NFVFID equations exactly. Therefore the numerical solution of these problems is very important. However, there are a few methods for solving these equations, numerically, and most of these methods have been applied to the linear and non-fractional problems, see [11,12,13,14,15,16,17].

In this paper, we will introduce a new operational method, based on CAS wavelets and Block Pulse Functions (BPFs), to solve NFVFID equations. The method is based on reducing Eq. (1) to a system of algebraic equations by expanding the solution via CAS wavelets with unknown coefficients. The main characteristic of an operational method is to convert a differential equation into an algebraic one. This method does not only simplify the problem but also speeds up the computation. The sparse structure of the operational matrices will simplify the problem and reduce the solution procedure. It is considerable that, our method can be easily applied for solving Eq. (1), when $\alpha \in \mathbb{N}$.

The plan of this paper is as follows. In section 2, fractional integral and differentiation operators, CAS wavelets, Block Pulse Functions and some of their properties are introduced. Section 3 introduces function approximations via CAS wavelets and BPFs in the matrix forms. In Section 4, the CAS wavelet operational matrix of fractional integration is derived. In Section 5, the approximation of CAS wavelets and BPFs and their operational matrices are used to reduce Eq. (1) to a system of algebraic equations. The error analysis of the method is discussed in section 6. In section 7 some numerical examples are presented to show the convergence, accuracy and advantages of the proposed method with a comparison to other methods. There is a conclusion of the

whole work in section 8. In appendices A and B, some details of calculations related to sections 4 and 5, are given.

2. Preliminaries

In this section, we present some notations, definitions, and preliminaries that will be used in the rest of the paper.

2.1 Fractional Calculus

There are several definitions of a fractional derivative of order $\alpha > 0$. The two most commonly used definitions are the Riemann- Liouville and Caputo fractional derivative. Each definition uses Riemann- Liouville fractional integration and derivatives of whole order. The Riemann-Liouville fractional integration of order α is defined as:

$$I^{\alpha} f(x) = \frac{1}{\Gamma(\alpha)} \int_0^x (x-t)^{\alpha-1} f(x)dt, \ x > 0, I^0 f(x) = f(x),$$

and the Caputo fractional derivative of order α is defined as $D_*^{\alpha} f(x) = I^{m-\alpha} D^m f(x)$, where D^m is the ordinary integer differential operator of order m and $I^{m-\alpha}$ is the Riemann- Liouville integral operator of order $m-\alpha$ with $m-1 < \alpha \le m$.

The relationship between the Riemann- Liouville operator and the Caputo operator is given by the following lemma [18]:

Lemma 2.1 *If* $m-1 < \alpha \le m, m \in \mathbb{N}$, *then:*

$D_*^{\alpha} I^{\alpha} f(x) = f(x)$, *and:*

$$I^{\alpha} D_*^{\alpha} f(x) = f(x) - \sum_{k=0}^{m-1} f^{(k)}(0^+) \frac{x^k}{k!}, \ x > 0.$$

2.2 CAS Wavelets and Block Pulse Functions(BPFs)

Wavelets are special kinds of oscillatory functions with compact support that are constructed by using dilation and translation of a single function, called the mother wavelet, denoted by $\psi(x)$ and must satisfy in certain requirements. If the dilation parameter is a and translation parameter is b, then we have the following family of wavelets:

$$\psi_{a,b}(x) = |a|^{-1/2} \psi\left(\frac{x-b}{a}\right), \ a, b \in \mathbb{R}, a \ne 0. \quad (3)$$

The CAS wavelets employed in this paper, are defined as:

$$\psi_{n,m}(x) = \begin{cases} 2^{k/2} CAS_m(2^k x - n), & \text{if } \frac{n}{2^k} \le x < \frac{n+1}{2^k}; \\ 0 & \text{otherwise,} \end{cases}$$

where:

$$CAS_m(x) = cos(2m\pi x) + sin(2m\pi x),$$

and $n = 0,1,...,2^k - 1, k \in \mathbb{N} \cup \{0\}, m \in \mathbb{Z}.$

Let us introduce the following useful notation, corresponding to CAS wavelets:

$$\tilde{\psi}_{n,m}(x) = \begin{cases} 2^{k/2} CAS_m(n - 2^k x), & \text{if } \frac{n}{2^k} \le x < \frac{n+1}{2^k}; \\ 0 & \text{otherwise.} \end{cases}$$

Definition 2.1 *An m- set of Block Pulse Functions (BPFs) over the interval* $[0,T)$ *is defined as* [19]:

$$b_i(x) = \begin{cases} 1, & \text{if } \frac{iT}{m} \le x < \frac{(i+1)T}{m}; \\ 0 & \text{otherwise,} \end{cases} \quad i = 0,1,2,\ldots,m-1,$$

with a positive integer value for m. In this paper, it is assumed that $T = 1$, so BPFs are defined over $[0,1)$.

Now we explain some applicable properties of BPFs:

- *Disjointness*:

$$b_i(x) b_j(x) = \begin{cases} b_i(x), & i = j; \\ 0, & i \ne j. \end{cases} \quad (4)$$

- *Orthogonality*:

$$\int_0^1 b_i(x) b_j(x) dx = \begin{cases} 1/m, & i = j; \\ 0, & i \ne j. \end{cases} \quad (5)$$

- *Completeness*:

For every $f \in L^2([0,1))$, the sequence $\{b_i\}$ is complete if $\int b_i f = 0$ results in $f = 0$, almost everywhere.

Because of the completeness of $\{b_i(x)\}$, Parseval's identity holds, i.e. we have $\int_0^1 f^2(x)dx = \sum_{i=0}^{\infty} f_i^2 \| b_i(x) \|^2$, for every real bounded function $f(x) \in L^2([0,1))$, and:

$$f_i = m \int_0^1 b_i(x) f(x) dx. \quad (6)$$

- BPFs have compact supports, i.e.:

$$Supp(b_i(x)) = [\frac{i}{m}, \frac{i+1}{m}].$$

3. Function Approximation

The set of CAS wavelets forms an orthonormal basis for $L^2([0,1))$. This implies that any function $f(x)$ defined over $[0,1)$, can be expanded as:

$$\begin{aligned} f(x) &= \sum_{n=0}^{\infty} \sum_{m \in Z} c_{n,m} \psi_{n,m}(x) \\ &\cong \sum_{n=0}^{2^k-1} \sum_{m=-M}^{M} c_{n,m} \psi_{n,m}(x) \\ &= \mathbf{c}^T \mathbf{\Psi}(x), \end{aligned}$$

where $c_{n,m} = < f(x), \psi_{n,m}(x) > = \int_0^1 f(x) \psi_{n,m}(x) dx,$ and $< f, g >$ is the inner product of the functions f and g, $\mathbf{c}$ and $\mathbf{\Psi}$ are $2^k(2M+1) \times 1$-vectors given by:

$$\mathbf{c} = [c_{0,-M}, c_{0,-M+1}, \ldots, c_{0,M}, c_{1,-M}, \ldots, c_{1,M}, \ldots, c_{2^k-1,-M}, \ldots, c_{2^k-1,M}]^T,$$

$$\mathbf{\Psi}(x) = [\psi_{0,-M}, \psi_{0,-M+1}, \ldots, \psi_{0,M}, \psi_{1,-M}, \ldots, \psi_{1,M}, \ldots, \psi_{2^k-1,-M}, \ldots, \psi_{2^k-1,M}]^T.$$

Also from the orthogonality property of BPFs, it is possible to expand functions into their Block- Pulse series [19]. This means that for every $f(x) \in L^2([0,1))$, we have:

$$f(x) \cong \sum_{i=0}^{m-1} f_i b_i(x) = \mathbf{f}^T \mathbf{B}_m(x), \tag{7}$$

where:

$$\mathbf{f} = [f_0, f_1, \ldots, f_{m-1}]^T,$$

$$\mathbf{B}_m(x) = [b_0(x), b_1(x), \ldots, b_{m-1}(x)]^T,$$

such that f_i's, $i = 0,1,\ldots,m-1$, are obtained by Eq. (6).

From the above representation and disjointness property, it follows that:

$$\mathbf{B}_m(x)\mathbf{B}_m^T(x) = \begin{bmatrix} b_0(x) & 0 & \ldots & 0 \\ 0 & b_1(x) & \ddots & \vdots \\ \vdots & \ddots & \ddots & 0 \\ 0 & \ldots & 0 & b_{m-1}(x) \end{bmatrix}, \tag{8}$$

$$\mathbf{B}_m^T(x)\mathbf{B}_m(x) = 1,$$

and:

$$\mathbf{B}_m(x)\mathbf{B}_m^T(x)\mathbf{a} = \tilde{\mathbf{a}}\,\mathbf{B}_m(x), \tag{8}$$

where $\mathbf{a}$ is an m-vector and $\tilde{\mathbf{a}} = diag(\mathbf{a})$.

Moreover, we can clearly conclud that for every $m \times m$ matrix A:

$$\mathbf{B}_m^T(x) A \mathbf{B}_m(x) = \tilde{A}^T \mathbf{B}_m(x), \tag{9}$$

where $\tilde{A}$ is an m-vector with elements equal to the diagonal entries of matrix A.

Notation. From now on, we define $m' = 2^k(2M+1)$, where $k, M \in \mathbb{N} \cup \{0\}$.

4. Operational Matrix of Fractional Integration

There is a relationship between BPFs and CAS wavelets. Providing some calculations outlined in appendix A, we have found:

$$\mathbf{\Psi}(x) = \mathbf{\Phi}_{m' \times m'} \mathbf{B}_{m'}(x). \tag{10}$$

The Block Pulse operational matrix of fractional integration F^α is given as follows [20]:

$$(I^\alpha \mathbf{B}_{m'})(x) \cong \mathbf{F}^\alpha \mathbf{B}_{m'}(x), \tag{11}$$

where:

$$\mathbf{F}^\alpha = \frac{1}{m'^\alpha} \frac{1}{\Gamma(\alpha+2)} \begin{bmatrix} 1 & \xi_1 & \xi_2 & \xi_3 & \ldots & \xi_{m'-1} \\ 0 & 1 & \xi_1 & \xi_2 & \ldots & \xi_{m'-2} \\ 0 & 0 & 1 & \xi_1 & \ldots & \xi_{m'-3} \\ \vdots & \vdots & \ddots & \ddots & & \vdots \\ 0 & 0 & \ldots & 0 & 1 & \xi_1 \\ 0 & 0 & 0 & \ldots & 0 & 1 \end{bmatrix},$$

and $\xi_k = (k+1)^{\alpha+1} - 2k^{\alpha+1} + (k-1)^{\alpha+1}$.

Remark 4.1 *For $\alpha = 1$, $\mathbf{F}^\alpha$ is the BPF's operational matrix of integration.*

Let:

$$(I^\alpha \mathbf{\Psi}_{m'})(x) \cong \mathbf{P}^\alpha_{m' \times m} \mathbf{\Psi}_{m'}(x), \tag{12}$$

where matrix $\mathbf{P}^\alpha_{m' \times m'}$ is called the CAS wavelet operational matrix of fractional integration. Using Eqs. (11) and (12), we have:

$$(I^\alpha \mathbf{\Psi}_{m'})(x) \cong (I^\alpha \mathbf{\Phi}_{m' \times m'} \mathbf{B}_{m'})(x) = \mathbf{\Phi}_{m' \times m'} (I^\alpha \mathbf{B}_{m'})(x) \cong \mathbf{\Phi}_{m' \times m'} \mathbf{F}^\alpha \mathbf{B}_{m'}(x). \tag{13}$$

By Eqs. (13) and (14), we get:

$$\mathbf{P}^\alpha_{m' \times m'} \mathbf{\Psi}_{m'}(x) \cong \mathbf{\Phi}_{m' \times m'} \mathbf{F}^\alpha \mathbf{B}_{m'}(x).$$

Therefore, the CAS wavelet operational matrix of fractional integration $\mathbf{P}^\alpha_{m' \times m'}$ is given by:

$$\mathbf{P}^\alpha_{m' \times m'} = \mathbf{\Phi}_{m' \times m'} \mathbf{F}^\alpha \mathbf{\Phi}^{-1}_{m' \times m'}.$$

5. Analysis of the Method

Consider Eq. (1), two variables functions $k_r(x,t) \in L^2([0,1))^2$, $r = 1,2$, can be approximated as:

$$k_r(x,t) \cong \sum_{n=0}^{2^k-1} \sum_{l_1=-M}^{M} \sum_{m=0}^{2^k-1} \sum_{l_2=-M}^{M} kr_{i,j} \psi_{n,l_1}(x) \psi_{m,l_2}(t),$$

for $i = n(2M+1) + l_1 + M + 1$, $j = m(2M+1) + l_2 + M + 1$, or in the matrix form:

$$k_r(x,t) \cong \mathbf{\Psi}^T(x) \mathbf{K}_\mathbf{r} \mathbf{\Psi}(t), \tag{14}$$

where $\mathbf{K}_\mathbf{r} = [kr_{i,j}]$ and $kr_{i,j} = <\psi_{n,l_1}(x), <k_r(x,t), \psi_{m,l_2}(t)>>$, for $r = 1,2$. The right hand side of Eq. (1) can also be written as:

$$g(x) \cong \mathbf{g}^T \mathbf{\Psi}(x). \tag{15}$$

Remark 5.1 *CAS wavelets cannot be used directly for solving differential equations because of their discontinuities. There are two possible ways to overcome this problem. The first possibility is converting the underlying differential equation into an equivalent integral equation and approximating the solution by truncated orthogonal CAS series and using operational matrices of integration to eliminate the integral operators. The second possibility is to expand the highest derivative term, appearing in the differential equation, into the CAS wavelet series.*

So, let:

$$D_*^{\alpha} f(x) \cong \mathbf{c}^T \mathbf{\Psi}(x). \quad (16)$$

By using lemma 2.1, Eqs. (13) and (17), we have:

$$f(x) \cong \mathbf{c}^T \mathbf{P}^{\alpha}_{m' \times m'} \mathbf{\Psi}(x) + \sum_{k=0}^{m-1} f^{(k)}(0^+) \frac{x^k}{k!}. \quad (17)$$

Hence, substituting the supplementary conditions (2) in (17) and approximating it via CAS walelets, we get:

$$f(x) \cong (\mathbf{c}^T \mathbf{P}^{\alpha}_{m' \times m'} + \mathbf{c_1}^T) \mathbf{\Psi}(x), \quad (18)$$

where $\mathbf{c_1}$ is an m'-vector. According to Eq. (11):

$$f(x) \cong (\mathbf{c}^T \mathbf{P}^{\alpha}_{m' \times m'} + \mathbf{c_1}^T) \mathbf{\Phi}_{m' \times m'} \mathbf{B}_{m'}(x). \quad (19)$$

Define:

$$\mathbf{a} = [a_0, a_1, ..., a_{m'-1}] = (\mathbf{c}^T \mathbf{P}^{\alpha}_{m' \times m'} + \mathbf{c_1}^T) \mathbf{\Phi}_{m' \times m'}. \quad (20)$$

By some calculations which are mentioned in details in appendix B, we will have:

$$\int_0^1 k_1(x,t)[f(t)]^{q_1} dt \cong \frac{1}{m'} \mathbf{N} \mathbf{B}_{m'}(x), \quad (22)$$

and:

$$\int_0^x k_2(x,t)[f(t)]^{q_2} dt \cong \tilde{A}^T \mathbf{B}_{m'}(x), \quad (23)$$

where:

$$\mathbf{N} = (\mathbf{\Phi}^T_{m' \times m'} \mathbf{K_1} \mathbf{\Phi}_{m' \times m'} \tilde{\mathbf{a}}_{q_1})^T,$$

$$\tilde{\mathbf{a}}_q = [a_0^q, a_1^q, ..., a_{m'-1}^q],$$

and $\tilde{A}$ is an m-vector whose elements are equal to the diagonal entries of the following matrix:

$$A = \mathbf{\Phi}^T_{m' \times m'} \mathbf{K_2} \mathbf{\Phi}_{m' \times m'} diag(\tilde{\mathbf{a}}_{q_2}) \mathbf{F}^1.$$

Now by substituting approximations (16), (17), (22) and (23) into Eq. (1), we obtain:

$$\mathbf{c}^T \mathbf{\Phi}_{m' \times m'} \mathbf{B}_{m'}(x) - \lambda_1 \frac{1}{m'} \mathbf{N} \mathbf{B}_{m'}(x) - \lambda_2 \tilde{A}^T \mathbf{B}_{m'}(x) \cong \mathbf{g}^T \mathbf{\Phi}_{m' \times m'} \mathbf{B}_{m'}(x). \quad (23)$$

According to orthogonality of BPFs, we have the following nonlinear system of algebraic equations:

$$\mathbf{c}^T \mathbf{\Phi}_{m' \times m'} - \lambda_1 \frac{1}{m'} \mathbf{N} - \lambda_2 \tilde{A}^T \cong \mathbf{g}^T \mathbf{\Phi}_{m' \times m'}. \quad (24)$$

By solving this system, with respect to the unknown vector $\mathbf{c}^T$, the approximate solution of Eq. (1) will be obtained according to Eq. (17).

6. Error Analysis

Theorem 6.1 [21] *A function $f(x) \in L^2[0,1]$, with bounded second derivative, say $\|f''(x)\| \le N$, can be expanded as an infinite sum of CAS wavelets, and the corresponding series converges uniformly to $f(x)$, that is:*

$$f(x) = \sum_{n=0}^{\infty} \sum_{m \in Z} c_{n,m} \psi_{n,m}(x)$$

We can easily check the accuracy of the method. Since the truncated CAS wavelet series is an approximate solution of Eq. (1), the resulting equation, (24), must be satisfied approximately in the main equation, that is for $x \in [0,1)$:

$$R_{m'}(x) = | \mathbf{c}^T \mathbf{\Phi}_{m' \times m'} \mathbf{B}_{m'}(x) - \lambda_1 \frac{1}{m'} \mathbf{N} \mathbf{B}_{m'}(x) - \lambda_2 \tilde{A}^T \mathbf{B}_{m'}(x) - \mathbf{g}^T \mathbf{\Phi}_{m' \times m'} \mathbf{B}_{m'}(x) | \cong 0.$$

Set $x = x_i$, our aim is to have $R_{m'}(x_i) \le 10^{r_i}$, where r_i is any positive integer. If we prescribe $Max\{r_i\} = 10^r$, then we increase m' as long as the following inequality holds at each point x_r:

$$R_{m'}(x_i) \le 10^r,$$

in other words, by increasing m' the error function $R_{m'}(x_i)$ approaches to zero.

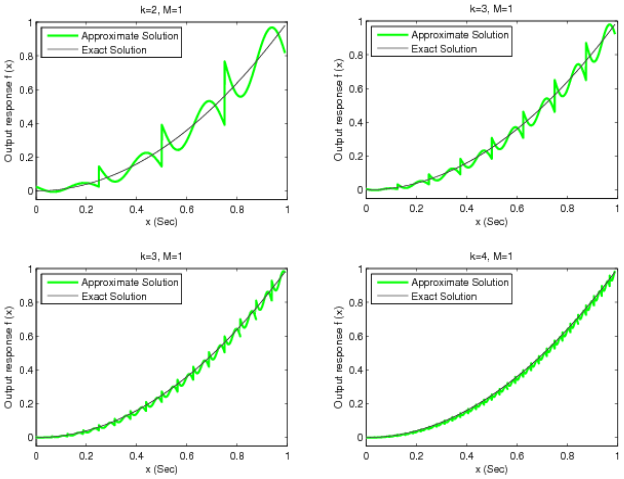

Figure 1. The comparison between approximate and exact solutions of Exmple 7.1 for some k and M, with $\alpha = 1$.

7. Numerical Examples

To illustrate the effectiveness of the proposed method, several test examples are carried out in this section. Note that:

$$\|e_{m'}(x)\|_2 = (\int_0^1 e^2_{m'}(x)dx)^{1/2} \cong (\frac{1}{N} \sum_{i=0}^{N} e^2_{m'}(x_i))^{1/2},$$

where $e_{m'}(x_i) = f(x_i) - f_{m'}(x_i)$, $i = 0,1,...,N$, $f(x)$ is the exact solution and $f_{m'}(x)$ is the approximate solution which is obtained by Eq. (17).

The computations associated with the examples were performed using Matlab on a Personal Computer.

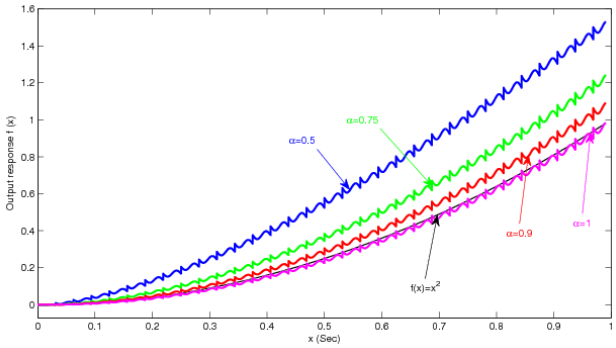

Figure 2. The comparison between approximate solutions of Exmple 7.1 for some $0.5 \le \alpha \le 1$, with $k = 5$ and $M = 1$.

Example 7.1 Error! Reference source not found. *Consider a NFVFID equation, as follows:*

$$D_*^{\alpha} f(x) - \frac{1}{4}\int_0^1 t f^3(t)dt + \frac{1}{2}\int_0^x x f^2(t)dt = g(x), \quad (25)$$

where $g(x) = \frac{x^6}{10} + 2x - \frac{1}{10}$, with the initial condition $f(0) = 0$, and the exact solution $f(x) = x^2$, in the case $\alpha = 1$. A comparison between the CAS wavelets solutions with some k and M, beside the approximate solutions and the exact solutions, are shown in Figure 1. Also, Figure 2 shows the numerical results for $k = 4, M = 1$ and various $0 < \alpha \le 1$. The comparisons show that as $\alpha \to 1$, the approximate solutions tend to $f(x) = x^2$, which is the exact solution of the equation in the case $\alpha = 1$. Table 2 presents the 2-norm of the absolute error in the case of $\alpha = 1$.

Example 7.2 [22-23] *For the following nonlinear integro-differential equation:*

$$D^{\alpha} f(x) + \int_0^x 3\cos(x-t) f^2(t)dt = \sin(2x), \quad (26)$$

with the initial condition $f(0) = 1$, and in the case $\alpha = 1$ the exact solution is $f(x) = \cos(x)$. Table 2 presents the comparison of the numerical solutions with the presented solution and figure 3 gives a comparison between the approximate solutions and the exact solution with some k and M.

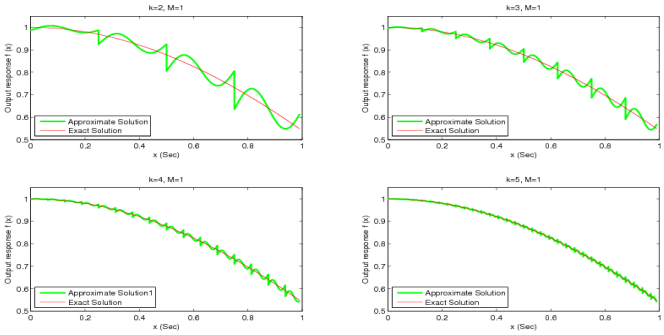

Figure 3. The comparison between approximate and exact solutions of Exmple 7.2 for some k and M, with $\alpha = 1$.

Table 1. The comparison between the approximate solutions and the exact solution (Example 7.3)

x	Exact solution	Presented method (k=4,M=1)	Presented method (k=5,M=1)	BPFs method [22] (m=16)	Adomian's method [23] (m=16)
0.0	1.000000	0.999210	0.999803	1.000000	1.000000
0.1	0.995004	0.994216	0.995507	0.995141	0.994951
0.2	0.980067	0.982054	0.981213	0.975784	0.980303
0.3	0.955336	0.952894	0.953794	0.960386	0.955685
0.4	0.921061	0.925488	0.919364	0.918443	0.921165
0.5	0.877583	0.861828	0.869898	0.862193	0.877048
0.6	0.825336	0.819314	0.827871	0.828963	0.822596
0.7	0.764842	0.770616	0.768348	0.752929	0.755333
0.8	0.696707	0.690310	0.692816	0.710418	0.667739
0.9	0.621610	0.630059	0.618108	0.617232	0.547241
1.0	0.540302	0.549002	0.542915	0.566917	0.364798

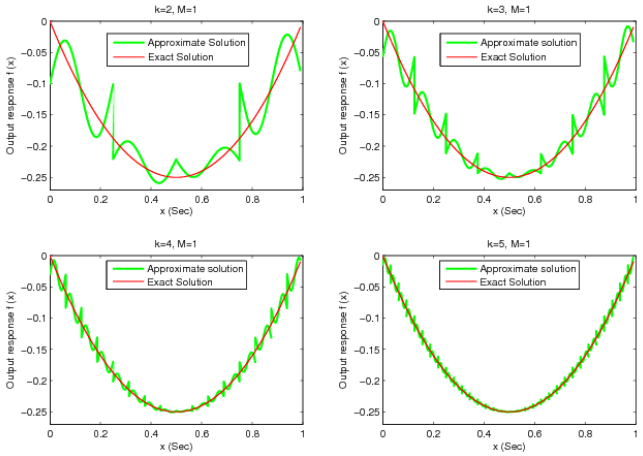

Figure 4. The comparison between approximate and exact solutions of Exmple 7.3 for some k and M.

Example 7.3 *Consider the following nonlinear integro-differential equation:*

$$D^{\frac{1}{2}} f(x) - \int_0^1 xt[f(t)]^4 dt - \int_0^x [f(t)]^2 = g(x), \quad (27)$$

where: $g(x) = \frac{1}{\Gamma(\frac{1}{2})}(\frac{8}{3}\sqrt{x^3} - 2\sqrt{x}) - \frac{x}{1260} - \frac{x^3(6x^2 - 15x + 10)}{30}$,

with the initial condition $f(0) = 0$, and the exact solution $f(x) = x^2 - x$. Table 1 and figure 4 show the comparison between the approximate solutions and the exact solution.

Table 2. The 2-norm of the absolute error.

Examples	$\|E\|_2, (k=3, M=1)$	$\|E\|_2, (k=4, M=1)$	$\|E\|_2, (k=5, M=1)$
Example 7.1 ($\alpha = 1$)	1.693401e-005	2.689175e-006	9.968712e-008
Example 7.2 ($\alpha = 1$)	1.001033e-005	2.498805e-006	6.243634e-007
Example 7.3	1.814125e-004	9.614030e-005	4.942423e-005
Example 7.4	1.184921e-004	6.636244e-005	3.507248e-005

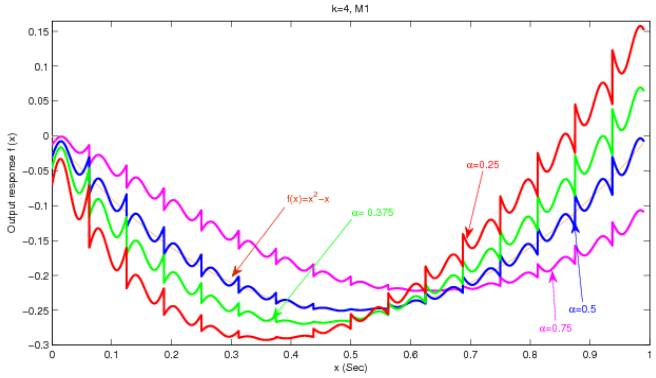

Figure 5. The comparison between approximate solutions of Exmple 7.3 for some $0.25 \le \alpha \le 0.75$.

Example 7.4 *For the following nonlinear integro-differential equation:*

$$f^{(4)}(x) - \int_0^1 (x+t)^2 f^3(t)dt - \int_0^x x^2 t f^2(t)dt = g(x), \qquad (28)$$

where:

$$g(x) = -\frac{x^{10}}{8} + \frac{3x^9}{7} - \frac{5x^8}{8} + \frac{x^7}{2} - \frac{15x^6}{64} + \frac{x^5}{16} - \frac{x^4}{128} - \frac{x}{5632} - \frac{1}{11264},$$

with the initial conditions $f(0) = -\frac{1}{8}, f'(0) = \frac{3}{4}$, $f''(0) = -3, f'''(0) = 6$ and the exact solution $f(x) = (x - \frac{1}{2})^3$, the comparison between the CAS wavelets method, with different values of k and M, beside the exact solutions, are shown in table 3 and figure 4.

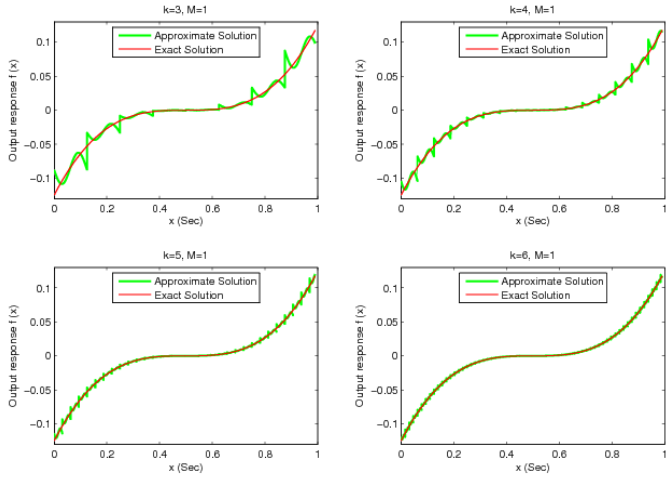

Figure 6. The comparison between approximate and exact solutions of Exmple 7.4 for some k and M.

8. Conclusion

A numerical scheme, based on operational matrices of integration for CAS wavelets and BPFs, transforms a fractional nonlinear Volterra-Fredholm integro-differential equation to a set of algebraic equations without applying any projection method. Solving this system by an iterative method gives an approximate solution which is a linear combination of $m = 2^k(2M+1)$ CAS wavelets. The applicability and accuracy of the method are checked by some examples. In these examples the approximate solutions are briefly compared with the exact and approximate solutions obtained by the other methods.

Increasing the number of CAS wavelets over $[0,1)$, decreases the error of the solution rapidly. To show its convergence and stability, the current method can be run with increasing m, until the computed results have appropriate accuracy. The advantage of this method is the low cost of setting up the equations without using any projection or collocation method and integration. The most interesting ability of this method is that, it can be simply applied to the cases where α is integer which is observed in the numerical examples.

Appendix A: Expanding CAS Wavelets Via BPFs

First, let us introduce the following useful notation, corresponding to CAS wavelets:

$$\tilde{\psi}_{n,m}(x) = \begin{cases} 2^{k/2} CAS_m(n - 2^k x), & \text{if } \frac{n}{2^k} \le x < \frac{n+1}{2^k}; \\ 0, & \text{otherwise.} \end{cases}$$

Eq. (7) implies that CAS wavelets can be also expanded into an m'-term BPF as:

$$\psi_{nm}(x) \cong \sum_{i=0}^{m'-1} f_i b_i(x).$$

By using the properties of CAS wavelets and Eq. (6), we get:

$$f_i = m' \int_{i/m'}^{(i+1)/m'} \psi_{nm}(x)dx$$

$$= \frac{m'}{2^{k+1} m\pi} \{\tilde{\psi}_{nm}(\frac{i}{m'}) - \tilde{\psi}_{nm}(\frac{i+1}{m'})\},$$

for:

$$i = n(2M+1), \ldots, n(2M+1) + (M-1), n(2M+1) + (M+1), \ldots, (n+1)(2M+1) - 1.$$

Note that for $i = n(2M+1) + M$, we have $f_i = 2^{k/2}$ and otherwise $f_i = 0$. Therefor, we get:

$$\psi_{nm}(x) \cong \frac{m'}{2^{k+1} m\pi} [\underbrace{0,0,\ldots,0}_{n(2M+1)}, \tilde{\psi}_{nm}(\frac{i}{m'}) - \tilde{\psi}_{nm}(\frac{i+1}{m'}), \ldots, \tilde{\psi}_{nm}(\frac{i+2M}{m'}) - \tilde{\psi}_{nm}(\frac{i+2M+1}{m'}),$$

$$0, \ldots, 0] \mathbf{B}_{m'}(x),$$

where $i = n(2M+1)$, $n = 0,1,\ldots,2^k - 1$ and $m = -M, \ldots, M$.

Hence:

$$\mathbf{\Psi}(x) = \mathbf{\Phi}_{m' \times m'} \mathbf{B}_{m'}(x), \qquad (29)$$

such that $\mathbf{\Phi}_{m' \times m'} = Diag(\mathbf{\Phi}_0, \mathbf{\Phi}_1, \ldots, \mathbf{\Phi}_{2^k - 1})$, and $\mathbf{\Phi}_n$ for $n = 0,1,\ldots,2^k - 1$ is a $(2M+1) \times (2M+1)$ matrix which is introduced as:

$$\mathbf{\Phi}_n = \Lambda \left(\begin{bmatrix} \tilde{\Psi}_n(\frac{i}{m'}) & \tilde{\Psi}_n(\frac{i+1}{m'}) & \ldots & \tilde{\Psi}_n(\frac{i+2M}{m'}) \end{bmatrix} - \begin{bmatrix} \tilde{\Psi}_n(\frac{i+1}{m'}) & \tilde{\Psi}_n(\frac{i+2}{m'}) & \ldots & \tilde{\Psi}_n(\frac{i+2M+1}{m'}) \end{bmatrix} \right),$$

here:

$$\Lambda = \frac{m'}{2^{k+1}\pi}\begin{bmatrix} \frac{1}{-M} & \frac{1}{-M+1} & \cdots & \frac{1}{-1} & \frac{2^{3k/2+1}\pi}{m'} & \frac{1}{-1} & \cdots & \frac{1}{M} \\ \frac{1}{-M} & \frac{1}{-M+1} & \cdots & \frac{1}{-1} & \frac{2^{3k/2+1}\pi}{m'} & \frac{1}{-1} & \cdots & \frac{1}{M} \\ \vdots & \vdots & \vdots & \vdots & & \vdots & \vdots & \vdots \\ \frac{1}{-M} & \frac{1}{-M+1} & \cdots & \frac{1}{-1} & \frac{2^{3k/2+1}\pi}{m'} & \frac{1}{-1} & \cdots & \frac{1}{M} \end{bmatrix},$$

$$\tilde{\boldsymbol{\Psi}}_n(x) = \begin{bmatrix} \tilde{\psi}_{n,-M}(x) & \tilde{\psi}_{n,-M+1}(x) & \cdots & \tilde{\psi}_{n,M}(x) \end{bmatrix}^T.$$

Appendix B: Expanding the Integral Part of the Main Equation Via CAS Wavelets

According to Eqs. (19) and (20), we have $f(x) \cong \mathbf{a}\,\mathbf{B}_{m'}(x)$. From the disjoint property of the BPFs, we get:

$$\begin{aligned}[f(x)]^2 &\cong [\mathbf{a}\,\mathbf{B}_{m'}(x)]^2 \\ &= [a_0 b_0(x) + a_1 b_1(x) + \ldots + a_{m'-1} b_{m'-1}(x)]^2 \\ &= a_0^2 b_0(x) + a_1^2 b_1(x) + \ldots + a_{m'-1}^2 b_{m'-1}(x) \\ &= \tilde{\mathbf{a}}_2 \mathbf{B}_{m'}(x),\end{aligned}$$

where $\tilde{\mathbf{a}}_2 = [a_0^2, a_1^2, \ldots, a_{m'-1}^2]$.

It is easy to show by induction that:

$$[f(x)]^q \cong [a_0^q, a_1^q, \ldots, a_{m'-1}^q]\mathbf{B}_{m'}(x) = \tilde{\mathbf{a}}_q \mathbf{B}_{m'}(x), \quad (30)$$

where:

$$\tilde{\mathbf{a}}_q = [a_0^q, a_1^q, \ldots, a_{m'-1}^q], \quad (31)$$

Using Eqs. (11), (15) and (31), we will have:

$$\int_0^1 k_1(x,t)[f(t)]^{q_1} dt = \int_0^1 \boldsymbol{\Psi}^T(x)\mathbf{K}_1\boldsymbol{\Psi}(t)\mathbf{B}_{m'}^T(t)\tilde{\mathbf{a}}^T{}_{q_1}\, dt$$

$$= \int_0^1 \boldsymbol{\Psi}^T(x)\mathbf{K}_1\boldsymbol{\Phi}_{m'\times m'}\mathbf{B}_{m'}(t)\mathbf{B}_{m'}^T(t)\tilde{\mathbf{a}}^T{}_{q_1}\, dt$$

$$= \boldsymbol{\Psi}^T(x)\mathbf{K}_1\boldsymbol{\Phi}_{m'\times m'}\int_0^1 \mathbf{B}_{m'}(t)\mathbf{B}_{m'}^T(t)\tilde{\mathbf{a}}^T{}_{q_1}\, dt. \quad (33)$$

Applying properties (4) and (5), we simplify the integral part of (33) as:

$$\int_0^1 \mathbf{B}_{m'}(t)\mathbf{B}_{m'}^T(t)\tilde{\mathbf{a}}^T{}_{q_1}\, dt = \int_0^1 \left\{ \begin{bmatrix} b_0(t) & & O \\ & b_1(t) & \\ & \ddots & \\ O & & b_{m'-1}(t) \end{bmatrix} \begin{bmatrix} a_0^{q_1} \\ a_1^{q_1} \\ \vdots \\ a_{m'-1}^{q_1} \end{bmatrix} \right\} dt$$

$$= \int_0^1 [a_0^{q_1} b_0(t), a_1^{q_1} b_1(t), \ldots, a_{m'-1}^{q_1} b_{m'-1}(t)]^T dt$$

$$= \frac{1}{m'}[a_0^{q_1}, a_1^{q_1}, \ldots, a_{m'-1}^{q_1}]^T$$

$$= \frac{1}{m'}\tilde{\mathbf{a}}^T{}_{q_1}.$$

Thus in (33), we have:

$$\int_0^1 k_1(x,t)[f(t)]^{q_1} dt \cong \frac{1}{m'}\boldsymbol{\Psi}^T(x)\mathbf{K}_1\boldsymbol{\Phi}_{m'\times m'}\tilde{\mathbf{a}}^T{}_{q_1}, \quad (34)$$

or:

$$\begin{aligned}\int_0^1 k_1(x,t)[f(t)]^{q_1} dt &\cong \frac{1}{m'}\mathbf{B}_{m'}^T(x)\boldsymbol{\Phi}_{m'\times m'}^T\mathbf{K}_1\boldsymbol{\Phi}_{m'\times m'}\tilde{\mathbf{a}}_{q_1} \\ &= \frac{1}{m'}(\boldsymbol{\Phi}_{m'\times m'}^T\mathbf{K}_1\boldsymbol{\Phi}_{m'\times m'}\tilde{\mathbf{a}}_{q_1})^T\mathbf{B}_{m'}(x) \\ &= \frac{1}{m'}\mathbf{N}\mathbf{B}_{m'}(x). \quad (35)\end{aligned}$$

Also the second integral part of Eq. (1), by the following process, can be written via CAS wavelets. Using Eqs. (11), (15) and (31), we will have:

$$\int_0^x k_2(x,t)[f(t)]^{q_2} dt = \int_0^x \boldsymbol{\Psi}^T(x)\mathbf{K}_2\boldsymbol{\Psi}(t)\mathbf{B}_{m'}^T(t)\tilde{\mathbf{a}}^T{}_{q_2}\, dt$$

$$= \int_0^x \boldsymbol{\Psi}^T(x)\mathbf{K}_2\boldsymbol{\Phi}_{m'\times m'}\mathbf{B}_{m'}(t)\mathbf{B}_{m'}^T(t)\tilde{\mathbf{a}}^T{}_{q_2}\, dt$$

$$= \boldsymbol{\Psi}^T(x)\mathbf{K}_2\boldsymbol{\Phi}_{m'\times m'}\int_0^x \mathbf{B}_{m'}(t)\mathbf{B}_{m'}^T(t)\tilde{\mathbf{a}}^T{}_{q_2}\, dt. \quad (33)$$

Using Eq. (8), we simplify the integral part of (36) as:

$$\int_0^x \mathbf{B}_{m'}(t)\mathbf{B}_{m'}^T(t)\tilde{\mathbf{a}}^T{}_{q_2}\, dt = \int_0^x diag(\tilde{\mathbf{a}}_{q_2})\mathbf{B}_{m'}(t)dt$$

$$= diag(\tilde{\mathbf{a}}_{q_2})\int_0^x \mathbf{B}_{m'}(t)dt$$

$$= diag(\tilde{\mathbf{a}}_{q_2})\mathbf{F}^1\mathbf{B}_{m'}(x).$$

Thus in (36), we get:

$$\int_0^x k_2(x,t)[f(t)]^{q_2} dt \cong \boldsymbol{\Psi}^T(x)\mathbf{K}_2\boldsymbol{\Phi}_{m'\times m'}diag(\tilde{\mathbf{a}}_{q_2})\mathbf{F}^1\mathbf{B}_{m'}(x)$$

$$= \mathbf{B}_{m'}^T(x)\boldsymbol{\Phi}_{m'\times m'}^T\mathbf{K}_2\boldsymbol{\Phi}_{m'\times m'}diag(\tilde{\mathbf{a}}_{q_2})\mathbf{F}^1\mathbf{B}_{m'}(x) = \tilde{A}^T\mathbf{B}_{m'}(x), \quad (34)$$

where $\tilde{A}$ is an m-vector with elements equal to the diagonal entries of the following matrix:

$$A = \boldsymbol{\Phi}_{m'\times m'}^T\mathbf{K}_2\boldsymbol{\Phi}_{m'\times m'}diag(\tilde{\mathbf{a}}_{q_2})\mathbf{F}^1.$$

Reference

[1] O. P. Agrawal, "A general formulation and solution scheme for fractional optimal control problems", *Nonlinear Dyn.*, vol. 38 , pp. 323–337, 2004.

[2] F. B. M. Duarte, J. A. Tenreiro Machado, "Chaotic phenomena and fractional-order dynamics in the trajectory control of redundant manipulators", *Nonlinear Dynamic*,. vol. 29, pp. 342–362, 2002.

[3] N. Engheta, "On fractional calculus and fractional multipoles in electromagnetism", *IEEE Transactions on Antennas and Propagation*, vol. 44, no. 4, pp. 554–566, 1996.

[4] R. L. Magin, "Fractional calculus models of complex dynamics in biological tissues", *Comput. Math. Appl.*, vol. 59, pp. 1586–1593, 2010.

[5] V. V. Kulish, J. L. Lage, "Application of fractional calculus to fluid mechanics", *J. Fluids Eng*, vol. 124, no. 3, pp. 803-806, 2002.

[6] K. B. Oldham, "Fractional differential equations in electrochemistry", *Advances in Engineering Software*, vol. 41, no.1, pp. 9–12, 2010.

[7] V. Gafiychuk, B. Datsko, V. Meleshko, "Mathematical modeling of time fractional reaction diffusion systems", *Computational and Applied Mathematics*, vol. 220, no. 1, pp. 215–225, 2008.

[8] C. Lederman, J-M Roquejoffre, N. Wolanski, "Mathematical justification of a nonlinear integrodifferential equation for the propagation of spherical flames", *Ann. di Mate.*, vol. 183, pp. 173–239, 2004.

[9] F. Mainardi, "Fractional calculus: some basic problems in continuum and statistical mechanics, in: A. Carpinteri, F. Mainardi (Eds.), Fractals and Fractional Calculus in Continuum Mechanics", *Springer-Verlag*, New York, pp. 291–348, 1997.

[10] F. C. Meral, T. J. Royston, "R. Magin, Fractional calculus in viscoelasticity: an experimental study", *Communications in Nonlinear Science and Numerical Simulation*, vol. 15, no. 4, pp. 939–945, 2010.

[11] M. A. Abdou, "Integral equation of mixed type and integrals of orthogonal polynomials", *J. Comput. Appl. Math.*, vol. 138, no. 2, pp. 273–285, 2002.

[12] M. A. Abdou, "On asymptotic methods for Fredholm–Volterra integral equation of the second kind in contact problems", *J. Comput. Appl. Math*., vol. 154, no. 2, pp. 431–446, 2003.

[13] E. Babolian, Z. Masouri, S. Hatamzadeh-Varmazyar, "Numerical solution of nonlinear Volterra–Fredholm integro-differential equations via direct method using triangular functions", *Comput. Math. Appl.*, vol. 58, no. 2, pp. 239–247, 2009.

[14] C. Cattani, "Shannon wavelets for the solution of integrodifferential equations", *mathematical problems in engineering*, pp. 1–22, 2010.

[15] C. H. Hsiao, "Hybrid function method for solving Fredholm and Volterra integral equations of the second kind", *Journal of Computational and Applied Mathematics*, vol. 230, no. 1, pp. 59–68, 2009.

[16] K. Maleknejad, M.Tavassoli Kajani, "Solving linear integro-differential equation system by Galerkin methods with hybrid functions", *Appl. Math. Comput.*, vol. 159, no. 3, pp. 603–612, 2004.

[17] A. M. Wazwaz, "The combined Laplace transform-Adomian decomposition method for handling nonlinear Volterra integro-differential equations", *Applied Mathematics and Computation*, vol. 216, no. 4, pp. 1304–1309, 2010.

[18] I. Podlubny, "Fractional Differential Equations'', *Academic Press*, New York, 1999.

[19] C. R. Rao, "Piecewise orthogonal functions and their applications on system and control'', *Springer*, Berlin, 1983.

[20] A. Kilicman, Z. Al Zhour "Kronecker operational matrices for fractional calculus and some applications". *Applied Mathematics and Computation*, vol 187, no. 1, pp. 250–265, 2007.

[21] H. Adibi, P. Assari, "Using CAS wavelets for numerical solution of Volterra integral equations of the second kind", *Dynamics of Continuous, Discrete and Impulsive Systems Series A: Mathematical Analysis*, vol. 16, no. 5, pp. 673–685, 2009.

[22] E. Babolian, Z. Masouri, S. Hatamzadeh-Varmazyar, "New direct method to solve nonlinear Volterra-Fredholm integral and integro differential equation using operational matrix with Block-pulse functions", Progress In *Electromagnetics Research B*, pp. 59-76, 2008.

[23] K. Maleknejad, M. Hadizadeh, "The numerical analysis of Adomian's decomposition method for nonlinear Volterra integral and integro-differential equations", *International Journal of Engineering Science*, Iran University of Science and Technology, vol. 8, no. 2a, pp. 33–48, 1997.